Inhibition of Cr(VI) in the Al2O3-CaO-Cr2O3 castables by using (Al1-x,Crx)2O3 solid solution

Tengteng Xu
Wuhan University of Science and Technology
Yibiao Xu (xuyibiao@wust.edu.cn)
Wuhan University of Science and Technology https://orcid.org/0000-0002-2293-1602
Yawei Li
Wuhan University of Science and Technology
Mithun Nath
Wuhan University of Science and Technology

Research Article

Keywords: Al2O3-CaO-Cr2O3 castables, (Al1-x,Crx)2O3 solid solution, Cr(VI) compounds, CA6, leaching test

Posted Date: December 10th, 2020

DOI: https://doi.org/10.21203/rs.3.rs-123797/v1

Abstract

Al_2O_3-CaO-Cr_2O_3 castables are required for various furnaces due to excellent corrosion resistance and sufficient early strength. However, generation of toxic Cr(VI) caused subsequent problems with disposal. The present work aimed at achieving Cr(VI) reduction by replacing Cr_2O_3 with $(Al_{1-x},Cr_x)_2O_3$ solid solution. The phase evolutions and Cr(VI) formation in castables were systemically investigated. Compared with Cr_2O_3, stability of $(Al_{1-x},Cr_x)_2O_3$ in CAC was much higher and improved gradually with Al^{3+} proportion. The substitution of Cr_2O_3 with $(Al_{1-x},Cr_x)_2O_3$ completely inhibited $CaCrO_4$ formation at 300–1100 ^oC, and drastically suppressed $Ca_4Al_6CrO_{16}$ generation at 900–1300 °C. Thus, a remarkable Cr(VI) reduction of 98.1% could be achieved. Moreover, In comparison with CA and CA_2, CA_6 was much more stable, which would not take chemical reaction with $(Al_{1-x},Cr_x)_2O_3$. Thus, incorporating some Al_2O_3 powders in Al_2O_3-CaO-Cr_2O_3 castables to form CA_6 at temperature above 1300 ^oC was also essential for inhibiting Cr(VI) formation when using $(Al_{1-x},Cr_x)_2O_3$ as substitute for Cr_2O_3.

1 Introduction

Al_2O_3-Cr_2O_3 refractories have high corrosion resistance due to the extremely low solubility and high chemical stability of Cr_2O_3 in molten slag, and are therefore widely used as lining materials in incinerators, gasifiers, glass furnaces and non-ferrous smelting, etc. [1–6]. Recently, the Al_2O_3-Cr_2O_3 refractories as castables are applied successfully since they are much more energy saving as well as convenient for installation and repairing compared with the bricks or shaped refractory products [7, 8]. During fabrication and application processes, binders play a key role in performance of the castables, of which calcium alumina cement (CAC, generally CA and CA_2 phases) is most widely used as it exhibits fast strength development and stable thermo-mechanical behavior, and even resistant to slag attack [9, 10]. However, the Cr_2O_3 can be oxidized into toxic Cr(VI) products at high temperature in the presence of alkali metal or alkaline earths metal oxides such as Na_2O, K_2O and CaO in oxidizing atmosphere [11–14]. Mithun et al investigated the phase evolution of the Al_2O_3-CaO-Cr_2O_3 castables after treatment at various temperature, and they found that CAC can facilitate the conversion of Cr(III) into Cr(VI) due to the presence of CaO [15]. Song and Garbers-Craig also confirmed that both CA and CA_2, as main phases of the CAC, can react with Cr_2O_3 in air to produce $Ca_4Al_6CrO_{16}$ (hauyne) at 1300 °C [16]. The Cr(VI) compounds poses a serious threat to the human and environment since they are toxic, carcinogenic and highly soluble in water [17, 18]. Therefore, it is of great environmental and practical significance to inhibit the Cr(VI) generation when applying Al_2O_3-CaO-Cr_2O_3 castables as lining materials.

Up till now, several research work focusing on the Cr(VI) formation and minimization have been carried out [19–21]. Generally, it was believed that the formation of Cr(VI) was closely related to atmosphere and basicity of other components in the Cr_2O_3 containing materials [22]. For the Cr_2O_3 containing refractory linings, since the operation conditions and service atmosphere in a given furnace can hardly be changed in practical production, most of the related work have focused on Cr(VI) minimization using some

additives at high temperatures. And the results suggested that acidic components such as SiO_2, TiO_2, Fe_2O_3 and P_2O_5 can effectively suppress the Cr(III) oxidation during thermal treatment of Cr_2O_3 containing refractories [4, 23–29]. However, these oxide additives usually result in formation of low melting point phases in the matrix, which would obviously deteriorate the thermo-mechanical properties or slag corrosion resistance of the refractories [30–32].

Previous research work indicated that incorporating chromium into spinel phases can also reduce the risk of Cr(VI) formation in the Cr_2O_3 containing materials [25, 33, 34]. For example, the investigation on the Al_2O_3-Cr_2O_3-CaO-MgO system confirmed that composite spinel $Mg(Al,Cr)_2O_4$ could co-exist with CA_2, where chromium existed in + 3 state [25, 34]. And for the magnesia-chrome refractories, adding a certain amounts of Al_2O_3 and TiO_2 can effectively lower the concentrations of Cr(VI) as chromium mainly exists in the form of $Mg(Al,Cr,Ti)_2O_4$ composite spinel [4]. Recent research work demonstrated that for the Al_2O_3-CaO-Cr_2O_3 castables, the CAC would facilitate the formation of very high concentrations of Cr(VI) compounds $CaCrO_4$ and $Ca_4Al_6CrO_{16}$ in air at mid-temperature (700–1100 ^oC), while nearly all the Cr_2O_3 would convert into $(Al_{1-x},Cr_x)_2O_3$ ($0 < x < 1$) solid solution at 1500 ^oC, which lead to significant decrease of Cr(VI) compounds amounts [23]. Again, our recent research work showed that the formation of glasses phases in the Al_2O_3-CaO-Cr_2O_3 castables could promote the $(Al_{1-x},Cr_x)_2O_3$ formation at high temperature, which drastically lowered the formation of Cr(VI) phases simultaneously [35]. These observations indicated that besides spinel phases, chromium existing in the form of $(Al_{1-x},Cr_x)_2O_3$ could probably reduce the risk of Cr(VI) formation in the Al_2O_3-CaO-Cr_2O_3 castables. The $(Al_{1-x},Cr_x)_2O_3$ is a substitutional solid solution with high refractoriness and good chemical stability, which could generally provide refractories with better performance like mechanical properties and slag corrosion resistance [36]. The investigation of the properties of Al_2O_3-CaO-Cr_2O_3 castables demonstrated that after firing at 1500 ^oC, corrosion resistance of the castables was improved obviously with Cr_2O_3 addition due to the enhanced formation of $(Al_{1-x},Cr_x)_2O_3$ solid solution [1]. Based on the above research, it can be inferred that substituting Cr_2O_3 with $(Al_{1-x},Cr_x)_2O_3$ solid solution as starting component in the Al_2O_3-CaO-Cr_2O_3 castables could be a feasible way to inhibit the formation of Cr(VI) at various temperature (especially at mid-temperature (700–1100 ^oC)) without compromising other properties. However, rarely any systematic work relating to the effect of $(Al_{1-x},Cr_x)_2O_3$ solid solution on Cr(VI) formation in Al_2O_3-CaO-Cr_2O_3 castables can be found publicly.

The present work aims to inhibit the formation of Cr(VI) compounds in Al_2O_3-CaO-Cr_2O_3 castables by substituting Cr_2O_3 with $(Al_{1-x},Cr_x)_2O_3$ solid solution as starting chromium containing constituent. Firstly, $(Al_{1-x},Cr_x)_2O_3$ solid solutions were pre-synthesized at 1300–1650 ^oC. Then, Al_2O_3-CaO-Cr_2O_3 castables with the pre-synthesized $(Al_{1-x},Cr_x)_2O_3$ solid solution were fabricated and treated at the temperature range of 300–1500 ^oC in air since castables would be put to use without firing and temperature gradient occurs in any furnace linings in actual practice. The phase evolution and Cr(VI) generation of the Al_2O_3-CaO-Cr_2O_3 castables with temperature and the corresponding mechanism were studied by means of XRD

and related software, SEM, and leaching tests. Furthermore, since the $(Al_{1-x},Cr_x)_2O_3$ could be formed in the Al_2O_3-CaO-Cr_2O_3 castables at high temperature [23], castables with Cr_2O_3 was pre-heated at 1500 ^oC to produce the in situ formed $(Al_{1-x},Cr_x)_2O_3$, whose effect on the Cr(VI) formation for the castables at various temperature was also eveluated.

2 Experimental

2.1 Fabrication of specimens

Tubular alumina ($w(Al_2O_3) \geq 98.6$ wt%, 5-3 mm, 3-1 mm, 1-0 mm, ≤ 0.045 mm, Zhejiang Zili Alumina Materials Technology Co. Lt., China), reactive α-alumina ($w(Al_2O_3) \geq 99.0$ wt%, ≤ 5 μm, Kaifeng Tenai Co. Ltd.), industrial grade fused chromium oxide ($w(Cr_2O_3) \geq 97.1$ wt%, ≤ 0.074 mm, Luoyang Yuda Refractories Co. Ltd.) and calcium aluminate cement namely Secar 71 (70.5 wt% Al_2O_3 and 29.0 wt% CaO, CA and CA_2 phases, Imerys aluminates, China) were used as starting materials for preparation of the castables. An organic defloculant, FS 65 (Sanndar Chemicals, China) was used as dispersant. Cr_2O_3 and Al_2O_3 fine powders with a mass ratio of 8:17 were dry-mixed and then treated at 1300 °C, 1600 °C and 1650 °C respectively for 3 h in air to obtain the pre-synthesized $(Al_{1-x},Cr_x)_2O_3$ solid solution, which were then pulverized to 200 mesh powders before adding into the castables. The specimen with Cr_2O_3 and Al_2O_3 powders as initial raw materials was labeled as C-R while specimens with $(Al_{1-x},Cr_x)_2O_3$ solid solution pre-synthesized at 1300 °C, 1600 °C and 1650 °C were labeled as C-S13, C-S16 and C-S165, respectively. Specimen C-R was pre-heated at 1500 ^oC for 3h (labeled as C-F15) to produce the in situ formed $(Al_{1-x},Cr_x)_2O_3$, whose effect on the Cr(VI) formation in the castables at various temperature was also eveluated then. The castables were formulated based on the Andreasen distribution co-efficient (q) value of 0.31. And the specific formulation is shown **Tab. 1**. Each batch was dry-mixed for 3 minutes in a Hobart mixer followed by wet-mixing (4.0wt% water, 25 °C) for further 3 minutes, and then castables were moulded in vibrating table (1 min) into bars of size 160 mm× 40 mm× 40 mm at room temperature. All specimens were cured at 25 °C and 75±5% relative humidity for 24 h in standrad cement maintainer, and dried at 110 °C for 24 h in an electric air oven after demoulding. Dried specimens C-R, C-S13, C-S16 and C-S165 togther with specimen C-F15 were finally heated in the temperature range of 300-1500 °C for 3h at peak temperature in air.

2.2 Characterization methods

The crystalline phase compositions were identified by X-ray diffraction (XRD) patterns using a PANalytical X'Pert Pro MPD diffractometer (copper Kα radiation (λ=1.5418Å) at 40 kV/40mA, step size 0.02 over a 2θ range of 5-90°) and analyzed by the software of Philips X'pert Pro High Score. Lattice parameters were calculated using Philips X'pert Pro High Score and Celref 2.0 software. Microstructure-morphology was analyzed by scanning electron microscopy (SEM, Nova 400 Nano-SEM, FEI Company, USA) equipped with energy dispersive spectroscopy (EDS, Oxford UK).

Cr(VI) leachability was evaluated using leaching test according to TRGS 613 standard procedure, which is suitable for the determination of water-soluble Cr(VI) compounds in cement and products containing cement [37]. Leaching specimens were prepared by crushing and grounding properly before passing through 200 mesh sieve (≤ 74μm). Fine specimens were stirred with deionized water as leaching solution using a magnetic stirrer at speed of 300 rpm for 15 minutes (at room temperature) with solid-liquid ratio of 1:20, and then leachates were obtained through a 0.45 μm membrane filter with a glass fiber by vacuum. The Cr(VI) concentration in the leachates was determined using a colorimetric method. The Cr(VI) can react in acid condition with the 1,5-diohenylcarbazide to form 1,5-diohenylcarbazone which is a red complex (0.02-0.2 mg/l chrome). Then the absorbance of the leachates after final treatment with 1,5-diphenylcarbazide (DPC) method was recorded at 540 nm, using a 722 Vis spectrophotometer (Jinghua Instruments, China).

3 Results

3.1 Pre-synthesis of $(Al_{1-x},Cr_x)_2O_3$ solid solution

XRD patterns of the pre-synthesized $(Al_{1-x},Cr_x)_2O_3$ solid solution specimens at different temperature were presented in **Fig. 1**. It could be found that both corundum and eskolaite existed as separate phases after dry mixing at 25 ^oC. After treated at 1300 ^oC, eskolaite disappeared completely with obvious reduction of the peak intensity of the corundum, while a new phase identified as $(Al_{1-x},Cr_x)_2O_3$ solid solution were generated. With the increase of the heat treatment temperature, the peak intensity of corundum reduced gradually until disappearance at 1650 ^oC, while the peak intensity of $(Al_{1-x},Cr_x)_2O_3$ solid solution increased steadily. After treated at temperatures up to 1650 ^oC, only $(Al_{1-x},Cr_x)_2O_3$ solid solution could be detected in the specimens. The 2θ value of the (012) peak of the $(Al_{1-x},Cr_x)_2O_3$ solid solution increased with the temperature (**Fig. 1b**), which demonstrated that more Al_2O_3 was dissolved into the $(Al_{1-x},Cr_x)_2O_3$ solid solution at higher temperature. To further investigate the crystal structure of the $(Al_{1-x},Cr_x)_2O_3$, the lattice parameters of the $(Al_{1-x},Cr_x)_2O_3$ solid solution at various temperature were calculated. As shown in **Tab. 2**, the lattice parameters decreased constantly with increasing the temperature. This was attributed to the fact that Al_2O_3 (reference code: JCPDS 01-081-2266, a=b=4.7569 Å and c=12.9830 Å) has lower lattice parameters than that of Cr_2O_3 (reference code: JCPDS 00-038-1479, a=b=4.9540 Å and c=13.5842 Å). Therefore, theoretically the decreasing trend of lattice parameters of $(Al_{1-x},Cr_x)_2O_3$ solid solution with an increase of Al_2O_3 dissolution at higher temperature was expected.

3.2 Cr(VI) leachability

The Cr(VI) concentration in Al_2O_3-CaO-Cr_2O_3 castables treated at various temperature was evaluated by leaching test according to the TRGS 613 standard procedure and the results are shown in **Fig. 2**. The details of Cr(VI) reduction compared to the reference specimen C-R is presented in **Table. 3**. It is revealed that with the addition of pre-synthesized $(Al_{1-x},Cr_x)_2O_3$ solid solution, a noticeable decrease in Cr(VI) concentration in the specimens was observed and specimens with $(Al_{1-x},Cr_x)_2O_3$ pre-synthesized at higher

temperature exhibited relative lower Cr(VI) concentration at the same heat treatment temperature (exception for specimen C-S165 at 1300 ^{o}C and 1500 ^{o}C). For example, at 700 ^{o}C, the total amount of Cr(VI) reduced drastically from 1233.2 mg/kg in specimen C-R (without $(Al_{1-x},Cr_x)_2O_3$) to 223.7 mg/kg in specimen C-S13 (a reduction of 81.9%), and reduced further to 24.0 mg/kg in specimen C-S165 (a reduction of 98.1%). However, at 1300 ^{o}C, specimen C-S165 exhibited even higher Cr(VI) concentration than that of reference specimen. Moreover, the temperature corresponding to the maximum Cr(VI) concentration shifted from 900 ^{o}C for specimen C-R to 1100 ^{o}C for the specimens with pre-synthesized $(Al_{1-x},Cr_x)_2O_3$. The specimen C-F15, which pre-heated at 1500 ^{o}C, exhibited extrememly low Cr(VI) concentration at all heat treatment temperatures studied. Although the mid-temperature (700-1100 ^{o}C) was favorable for the formation of Cr(VI), the total amount of Cr(VI) in specimen C-F15 at 700 ^{o}C-1300 ^{o}C was still only 13.0-17.3 mg/kg (a reduction of ~98.9%-99.1% compared to that of specimen C-R), which was below the allowable Cr(VI) limit values of Environmental Protection Agency (EPA), United States (5 mg/L equivalent to 100 mg/kg) [38].

3.3 Phase evolution of the castables

In order to study the effect of the pre-synthesized $(Al_{1-x},Cr_x)_2O_3$ solid solution on the phase evolution of the castables, phase compositions of the specimens treated at 110-1500 ^{o}C were analyzed and the results are shown in **Fig. 3**. It could be found that in all specimens, main phase corundum together with $NaAl_{11}O_{17}$ impurity could be detected at all temperatures, and hydrate phase C_3AH_6 was generated at 110 ^{o}C but then disappeared at 300 ^{o}C due to dehydration. For specimen C-R, $CaCrO_4$ phase could be detected at 300 ^{o}C, whose peak intensity increased with the increase of temperature from 300 to 900 °C but then decreased with further increasing temperature until disappearance at 1300 °C. The hauyne ($Ca_4Al_6CrO_{16}$) was generated at 900 ^{o}C, whose peak intensity reached a maximum at 1100 °C but dropped down with further increasing temperature until disappearance at 1500 °C. Moreover, eskolaite existing in the range of 110 °C to 1100 °C reduced in peak intensity with temperature and disappeared at 1300 °C, while $(Al_{1-x},Cr_x)_2O_3$ solid solution and $CaAl_{12}O_{19}$ (CA_6, calcium hexa-aluminate) increased in peak intensity after generating at 1100 °C and 1300 °C, respectively. However, for specimens C-S13, C-S16 and C-S165, no $CaCrO_4$ phase was detected at 300-1100 °C, indicating that chromium in the $(Al_{1-x},Cr_x)_2O_3$ solid solution would not be oxidized by the CAC in this temperature range. At 900-1300 °C, although the hauyne phase was still formed in these specimens with pre-synthesized $(Al_{1-x},Cr_x)_2O_3$, the peak intensity of this Cr(VI) compound was much lower compared with that in specimen C-R at the same temperature. The peak intensity of $Ca_4Al_6CrO_{16}$ phase reached the maximum at 1100 °C in Al_2O_3-CaO-Cr_2O_3 castables and therefore, the highest Cr(VI) concentration for the specimens with pre-synthesized $(Al_{1-x},Cr_x)_2O_3$ was detected at 1100 ^{o}C (**Fig. 2**). In general, the substitution of Cr_2O_3 with $(Al_{1-x},Cr_x)_2O_3$ in the Al_2O_3-CaO-Cr_2O_3 castables can almost completely restrict the formation of $CaCrO_4$ compound at 300-1100 °C and effectively lower the Cr(VI) compound $Ca_4Al_6CrO_{16}$ formation at 900-1300 °C, which was in accordance with the results of Cr(VI) leachability shown in **Fig. 2**. After treated at 1500 °C, only corundum (with

$NaAl_{11}O_{17}$ impurity), $(Al_{1-x},Cr_x)_2O_3$ solid solution and CA_6 phases was found in specimens C-R, C-S13, C-S16 and C-S165. Whereas, the enlarged XRD patterns of the castables in **Fig. 3c** indicated that specimens with $(Al_{1-x},Cr_x)_2O_3$ pre-synthesized at higher temperature exhibited relative lower peak intensity of CA_6 phase after treated at 1300 °C. Besides, the specimen C-F15, which had the same phase compositions as the other four specimens treated at 1500 °C, showed hardly any phase changes with the subsequent heat treatment temperature.

4 Discussion

The above results demnstrated that in the Al_2O_3-CaO-Cr_2O_3 castables, chromium and calcium would exist in the state of Cr_2O_3/$(Al_{1-x},Cr_x)_2O_3$ and CAC/CA_6 respectively, which apparently affected the formation and concentration of Cr(VI) compounds $CaCrO_4$ and hauyne at mid-temperature (700-1100 ^oC). In order to figure out the mechanisms of the Cr(VI) generation in the castables and the corresponding chemical reactions, fine powders of CAC/CA_6 were mixed with Cr_2O_3/$(Al_{1-x},Cr_x)_2O_3$ (pre-synthetized at 1650 ^oC) and then the mixed powders (formulation shown in **Tab. 4**) were pressed into Φ20 mm×20 mm cylindrical specimens under a pressure of 50 MPa. After treated at 900 ^oC and 1300 ^oC for 3 hours in air, the phase compositions and microstructures the of the specimens were analyzed by XRD (**Fig. 4**) and SEM (**Fig. 5**), respectively. And the plausible chemical reaction equations discussed below in various specimens heated at 900 ^oC and 1300 ^oC were list in **Tab. 5**.

After treated at 900 ^oC, the CA phase from CAC disappeared in specimen C-C with the formation of many granular $CaCrO_4$ grains (**Fig. 5a**) via reaction 1, whereas specimen C-S was still composed of the initial main phases (CA, CA_2 and $(Al_{1-x},Cr_x)_2O_3$) (**Fig. 5b**) in addition to forming minute amounts of hauyne (reaction 2). As the heat treatment temperature increased to 1300 ^oC, plenty of hauyne and $(Al_{1-x},Cr_x)_2O_3$ solid solution (**Fig. 5e**) were generated in specimen C-C (via reactions 3-5) accompanying with the disappearance of CA and significant reduction of CA_2 phase, while specimen C-S possessed relative lower peak intensity of hauyne although it had the same kind of phases as specimen C-C. Combining the observations of Cr(VI) in **Fig 2** with the phase evolution results (**Fig. 3 and Fig. 4**), it can be deduced that compared with Cr_2O_3, the $(Al_{1-x},Cr_x)_2O_3$ solid solution was more stable that would not form $CaCrO_4$ and could effectively hinder the hauyne formation when contacted with CAC, and therefore the substitution of Cr_2O_3 with $(Al_{1-x},Cr_x)_2O_3$ can effectively lower the Cr(VI) concentration of the castables after treated at various temperature (**Fig. 2**). The castables with $(Al_{1-x},Cr_x)_2O_3$ pre-synthesized at higher temperature exhibited lower Cr(VI) concentration, implying that the stability of the $(Al_{1-x},Cr_x)_2O_3$ improved gradually with the Al_2O_3 proportion in the solid solution. Besides, in comparison with CA_2 phase, CA was more likely to react with Cr_2O_3/$(Al_{1-x},Cr_x)_2O_3$ resulting in the formation of Cr(VI) compounds.

For specimens CH-C, no new phases were occurred after heat treatment at 900 ^oC, and only miniscule amount of hauyne was generated at 1300 ^oC (**Fig. 5g**) via Eqs. 6, which also produced Al_2O_3 that subsequently interacted with Cr_2O_3 to generate the $(Al_{1-x},Cr_x)_2O_3$ solid solution via Eqs. 5. It is worth

mentioning that no changes in the phase compositions were detected in specimen CH-S after heat treatment at both 900 ^{o}C and 1300 ^{o}C. These observations demonstrated that calcium in CA_6 was much more stable comparing with that in both CA and CA_2, which only caused slight oxidation of Cr_2O_3 and would not take chemical reaction with $(Al_{1-x},Cr_x)_2O_3$ solid solution. Therefore, specimen C-F15, in which chromium and calcium existed in $(Al_{1-x},Cr_x)_2O_3$ and CA_6 respectively, showed no changes in phase composition and extremely low Cr(VI) concentration at various heat treatment temperature. In the Al_2O_3-CaO-Cr_2O_3 castables, CA_6 could be generated from the reaction between CAC and Al_2O_3 powders in the matrix at 1300 ^{o}C (**Fig. 3**). However, for specimen C-S165, since no Al_2O_3 existed in the $(Al_{1-x},Cr_x)_2O_3$ powder pre-synthesized at 1650 ^{o}C (**Fig. 1**), the calcium would be still exist as CA and CA_2 rather than CA_6 at 1300 ^{o}C. As a result, specimen C-S165 possessed even higher Cr(VI) concentration than that of the reference specimen C-R at 1300 ^{o}C, attributing to the fact that CA and CA_2 can more easily react with $(Al_{1-x},Cr_x)_2O_3$ to produce hauyne compared with CA_6.

5 Conclusions

In the present work, $(Al_{1-x},Cr_x)_2O_3$ solid solution was pre-synthesized at different temperature, whose inhibition on the Cr(VI) formation in the Al_2O_3-CaO-Cr_2O_3 castables was systematically investigated. And the following conclusions can be drawn:

(1) Compared with Cr_2O_3, the stability of $(Al_{1-x},Cr_x)_2O_3$ solid solution in contact with CAC was much higher, which improved gradually with the proportion of Al_2O_3 in the solid solution. The substitution of Cr_2O_3 with $(Al_{1-x},Cr_x)_2O_3$ in the Al_2O_3-CaO-Cr_2O_3 castables can completely inhibit the mid-temperature (300–1100 ^{o}C) formation of Cr(VI) compound $CaCrO_4$, and relatively higher temperature Cr(VI) phase $Ca_4Al_6CrO_{16}$ (hauyne) drastically reduced at 900–1300 °C. Therefore, replacing Cr_2O_3 with $(Al_{1-x},Cr_x)_2O_3$ can effectively lower the Cr(VI) concentration of the castables after treated at various temperature and a reduction of Cr(VI) amounts up to 98.1% with $(Al_{1-x},Cr_x)_2O_3$ addition could be achieved.

(2) In comparison with CA_2 phase, CA was more likely to react with Cr_2O_3/$(Al_{1-x},Cr_x)_2O_3$ resulting in Cr(VI) compounds formation, while calcium in CA_6 was much more stable comparing with that in both CA and CA_2, which only caused slight oxidation of Cr_2O_3 and would not take chemical reaction with $(Al_{1-x},Cr_x)_2O_3$ solid solution. Thus, incorporating some Al_2O_3 powders in the matrix of the Al_2O_3-CaO-Cr_2O_3 castables to form CA_6 at temperature above 1300 ^{o}C was also essential for inhibiting Cr(VI) formation when using $(Al_{1-x},Cr_x)_2O_3$ solid solution as substitute for Cr_2O_3.

Declarations

Acknowledgements

This work was supported by the National Natural Science Foundation of China (NSFC) (Nos. 51950410587, 51872211 and U1908227).

References

1. Nath M, Song SQ, Li YW, et al. Effect of Cr_2O_3 addition on corrosion mechanism of refractory castables for waste melting furnaces and concurrent formation of hexavalent chromium. Ceram Int 2018, 44: 2383-2389.
2. Weinberg AV, Varona C, Chaucherie X, et al. Extending refractory lifetime in rotary kilns for hazardous waste incineration. Ceram Int 2016, 42: 17626-17634.
3. Kaneko TK, Zhu JX, Howell N, et al. The effects of gasification feedstock chemistries on the infiltration of slag into the porous high chromia refractory and their reaction products. Fuel 2014, 115: 248-263.
4. Xu TT, Xu YB, Li YW, et al. Corrosion mechanisms of magnesia-chrome refractories in copper slag and concurrent formation of hexavalent chromium. J Alloy Compd 2019, 786: 306-313.
5. Li JJ, Zhao HZ, Zhao PD, et al. Effects of Cr_2O_3 addition on property improvement of magnesia-spinel refractories used in RH snorkel. Ceram Int 2016, 42: 18579-18584.
6. Nath M, Ghosh A, Tripathi HS. Hot corrosion behavior of Al_2O_3-Cr_2O_3 refractory by molten glass at 1200 °C under static condition. Corros Sci 2016, 102: 153-160.
7. Tomšů F, Palčo S. Refractory Monolithics versus Shaped Refractory Products. Int Ceram Rev 2017, 66: 20-23.
8. Lee WE, Vieira W, Zhang S, et al. Castable refractory concretes. Int Mater Rev 2013, 46: 145-167.
9. Parr C, Roesky R, Wang YT, et al. High performance calcium aluminate cements for corrosion resistant castables. CSM Int Refract Confer 2001: 1-13.
10. Heikal M, Radwan MM, Al-Duaij OK. Physico-mechanical characteristics and durability of calcium aluminate blended cement subject to different aggressive media Build Mater 2015, 78: 379-385.
11. Mao LQ, Gao BY, Deng N, et al. Oxidation behavior of Cr(III) during thermal treatment of chromium hydroxide in the presence of alkali and alkaline earth metal chlorides. Chemosphere 2016, 145: 1-9.
12. Mao LQ, Gao BY, Deng N, et al. The role of temperature on Cr(VI) formation and reduction during heating of chromium-containing sludge in the presence of CaO. Chemosphere 2015, 138: 197-204.
13. Garcia-Ramos E, Romero-Serrano A, Zeifert B, et al. Immobilization of chromium in slags using MgO and Al_2O_3. Steel Res Int 2008, 79: 332-339.
14. Lee Y, Nassaralla CL. Formation of hexavalent chromium by reaction between slag and magnesite-chrome refractory. Matall Mater Trans B 1998, 29: 405-410.
15. Nath M, Song SQ, Garbers-Craig A, et al. Phase evolution with temperature in chromium-containing refractory castables used for waste melting furnaces and Cr(VI) leachability. Ceram Int 2018, 44: 20391-20398.

16. Song SQ, Andrie GC. Reaction between synthesized calcium aluminates and Cr_2O_3 in air and CO_2. Advances in Molten Slags, Fluxes, and Salts: Proceedings of the 10th International Conference on Molten Slags, Fluxes and Salts 2016.
17. Pradhan D, Sukla LB, Sawyer M, et al. Recent bioreduction of hexavalent chromium in wastewater treatment: A review. J Ind Eng Chem 2017, 55: 1-20.
18. Shanker AK, Venkateswarlu B. Chromium: Environmental Pollution Health Effects and Mode of Action. Environ Health 2011: 650-659.
19. Bishop ME, Glasser P, Dong HL, et al. Reduction and immobilization of hexavalent chromium by microbially reduced Fe-bearing clay minerals. Geochim Cosmochim Ac 2014, 133: 186-203.
20. Lee Y, Nassaralla C. Minimization of Hexavalent Chromium in Magnesite-Chrome refractory. Matall Mater Trans B 1997, 28B: 855-859.
21. Chen J, Jiao FC, Zhang L, et al. Elucidating the mechanism of Cr(VI) formation upon the interaction with metal oxides during coal oxy-fuel combustion. J Hazard Mater 2013, 261: 260-268.
22. Zhao PD, Zhang H, Yu J, et al. Conditions for mutual conversion of Cr(III) and Cr(VI) in aluminum chromium slag. J Alloy Compd 2019, 788: 506-513.
23. Nath M, Song SQ, Xu TT, et al. Effective inhibition of Cr(VI) in the Al_2O_3-CaO-Cr_2O_3 refractory castables system through silica gel assisted in-situ secondary phase tuning. J Clean Prod 2019, 233: 1038-1046.
24. Mao LQ, Deng N, Liu L, et al. Effects of Al_2O_3 Fe_2O_3 and SiO_2 on Cr(VI) formation during heating of solid waste containing Cr(III). Chem Eng J 2016, 304: 216-222.
25. Wu YJ, Song SQ, Garbers-Craig A, et al. Formation and leachability of hexavalent chromium in the Al_2O_3-CaO-MgO-Cr_2O_3 J Eur Ceram Soc 2018, 38: 2649-2661.
26. Warshaw I, Keith ML. Solid solution and chromium oxide loss in part of the system MgO-Al_2O_3-Cr_2O_3-SiO_2. J Am Ceram Soc 1954, 37: 161-168.
27. Mao LQ, Deng N, Liu L, et al. Inhibition of Cr(III) oxidation during thermal treatment of simulated tannery sludge: The role of phosphate. Chem Eng J 2016, 294: 1-8.
28. Wei YL, Hsieh HF, Yang YW, et al. Molecular study of thermal immobilization of chromium(VI) with clay. J Air Waste Manage 2005, 55: 411-414.
29. Lin SH, Chen CN, Juang RS. Structure and thermal stability of toxic chromium(VI) species doped onto TiO_2 powders through heat treatment. J Environ Manage 2009, 90: 1950-1955.
30. Martinez AGT, Luz AP, Braulio MAL, et al. Creep behavior modeling of silica fume containing Al_2O_3-MgO refractory castables. Ceram Int 2012, 38: 327-332.
31. Sako EY, Braulio MAL, Pandolfelli VC. The corrosion resistance of microsilica-containing Al_2O_3-MgO and Al_2O_3-spinel castables. Ceram Int 2012, 38: 4783-4789.
32. Bie CY, Sang SB, Li YW, et al. Effects of firing and operating atmospheres on microstructure and properties of phosphate bonded Cr_2O_3-Al_2O_3-ZrO_2 Refractories (CN) 2015, 49: 168-174.

33. Mao LQ, Tang RZ, Wang YC, et al. Stabilization of electroplating sludge with iron sludge by thermal treatment via incorporating heavy metals into spinel phase. J Clean Prod 2018, 187: 616-624.
34. Klyucharov YV, Eger VG. On the reaction between magnesiochromite and calcium oxide. Refractories 1963, 4: 3.
35. Xu TT, Liao N, Xu YB, et al. In situ detoxification and mechanical properties of Al_2O_3-Cr_2O_3-CaO castables with zeolite. J Eur Ceram Soc 2021, 41: 978-985.
36. Shibata K, Yoshinaka M, Hirota K, et al. Fabrication and mechanical properties of Cr_2O_3 solid solution ceramics in the system Cr_2O_3-Al_2O_3. Mater Res Bull 1997, 32: 627-632.
37. TRGS 613 The Technical Rules For Hazardous Substance. 2002.
38. Toxicological review of hexavalent chromium in: U.S. Environmental Protection Agency (EPA) No. 18540-29-9 USA Washington. 1998.

Tables

Tab. 1 The formulation of Al_2O_3-CaO-Cr_2O_3 castables (wt%)

Specimens	Al_2O_3 aggregates	Al_2O_3 fine powder	Cr_2O_3 fine powder	$(Al_{1-x},Cr_x)_2O_3$ solid solution (°C)			CAC	Dispersant
				1300	1600	1650		
C-R	70	17	8	-	-	-	5	0.1
C-S13	70	-	-	25			5	0.1
C-S16	70	-	-		25		5	0.1
C-S165	70	-	-	-	-	25	5	0.1
C-F15	70	17	8	-	-	-	5	0.1

Tab. 2 The lattice parameters of $(Al_{1-x},Cr_x)_2O_3$ solid solution pre-synthesized at different temperature. *Corundum* (JCPDS 01-081-2266) and Eskolaite# (JCPDS 00-038-1479)*

Pre-synthesized temperature	Phases	Lattice parameters (Å)	
		a=b	c
25 °C	Corundum*	4.7569	12.9830
	Eskolaite#	4.9540	13.5842
1300 °C	$(Al_{1-x},Cr_x)_2O_3$ solid solution	4.8607	13.2580
1600 °C		4.8291	13.1823
1650 °C		4.7576	12.9904

Tab. 3 Cr(VI) reduction (%) of specimens with $(Al_{1-x},Cr_x)_2O_3$ solid solution compared to specimen C-R at different temperatures

Specimens	Temperature (°C)							
	110	300	500	700	900	1100	1300	1500
C-S13	43.7	-19.5	61.7	81.9	16.1	21.2	10.5	12.6
C-S16	47.4	48.6	93.4	95.0	57.2	24.0	28.0	38.7
C-S165	38.5	58.0	87.4	98.1	67.6	35.8	-91.4	-202.4
C-F15	-	-	-	98.9	99.1	99.0	93.5	-30.8

Tab. 4 The formulation of cylindrical specimens (wt%)

Specimens	CAC	CA_6	Cr_2O_3	$(Al_{1-x},Cr_x)_2O_3$
C-C	50		50	
C-S	50			50
CH-C		50	50	
CH-S		50		50

Tab. 5 Chemical reaction equations in cylindrical specimens

Specimens	900 °C	1300 °C
C-C	(1)	(3) (4) (5)
C-S	(2)	(2)
CH-C	-	(5) (6)
CH-S	-	-

$4CaAl_2O_4+2Cr_2O_3+3O_2 \rightarrow 4CaCrO_4+4Al_2O_3$ (1)

$16CaAl_2O_4+y(Al_{1-x},Cr_x)_2O_3+3O_2 \rightarrow 4Ca_4Al_6CrO_{16}+(y+2)Al_2O_3$ (2)

$16CaAl_2O_4+2Cr_2O_3+3O_2 \rightarrow 4Ca_4Al_6CrO_{16}+4Al_2O_3$ (3)

$16CaAl_4O_7+2Cr_2O_3+3O_2 \rightarrow 4Ca_4Al_6CrO_{16}+20Al_2O_3$ (4)

$(1-x)Al_2O_3+xCr_2O_3 \rightarrow (Al_{1-x},Cr_x)_2O_3$ (5)

$16CaAl_{12}O_{19}+2Cr_2O_3+3O_2 \rightarrow 4Ca_4Al_6CrO_{16}+84Al_2O_3$ (6)

Figures

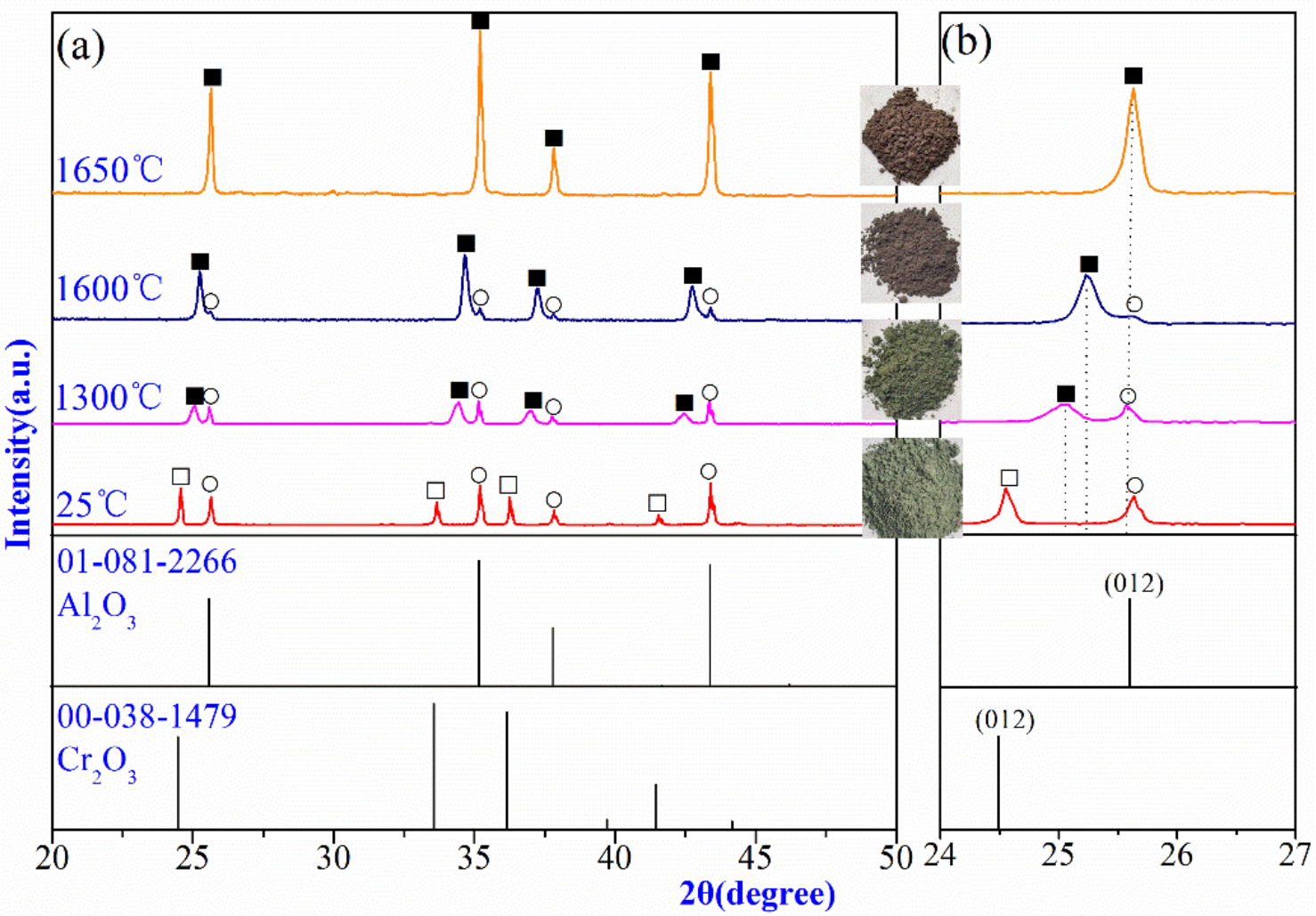

Figure 1

XRD pattern of (Al1-x,Crx)2O3 solid solution pre-synthesized at different temperature, (a) 2θ = 20-50°, (b) 2θ = 24-27°.

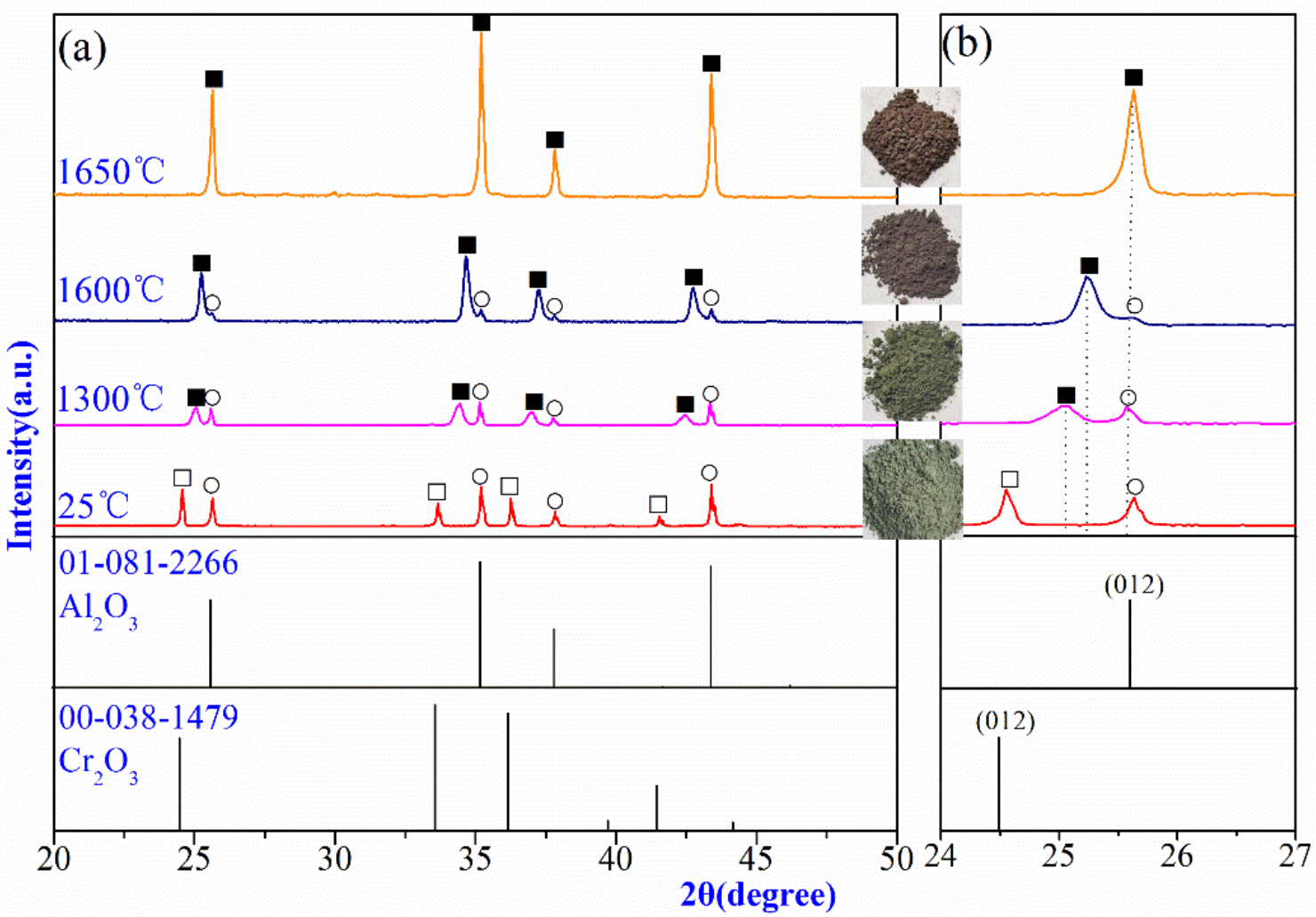

Figure 1

XRD pattern of (Al1-x,Crx)2O3 solid solution pre-synthesized at different temperature, (a) 2θ = 20-50°, (b) 2θ = 24-27°.

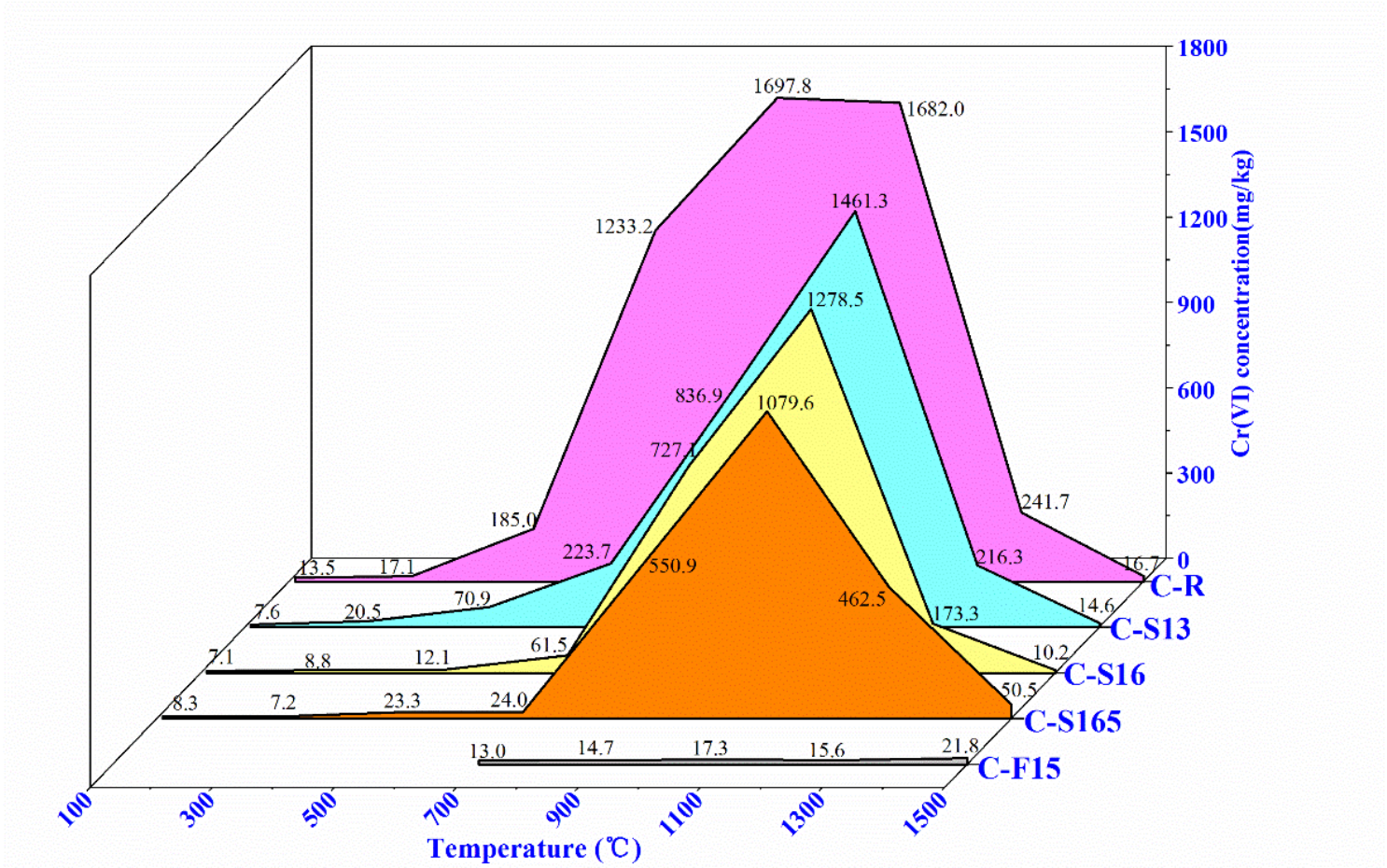

Figure 2

Cr(VI) concentration as a function of temperature in Al2O3-CaO-Cr2O3 castables.

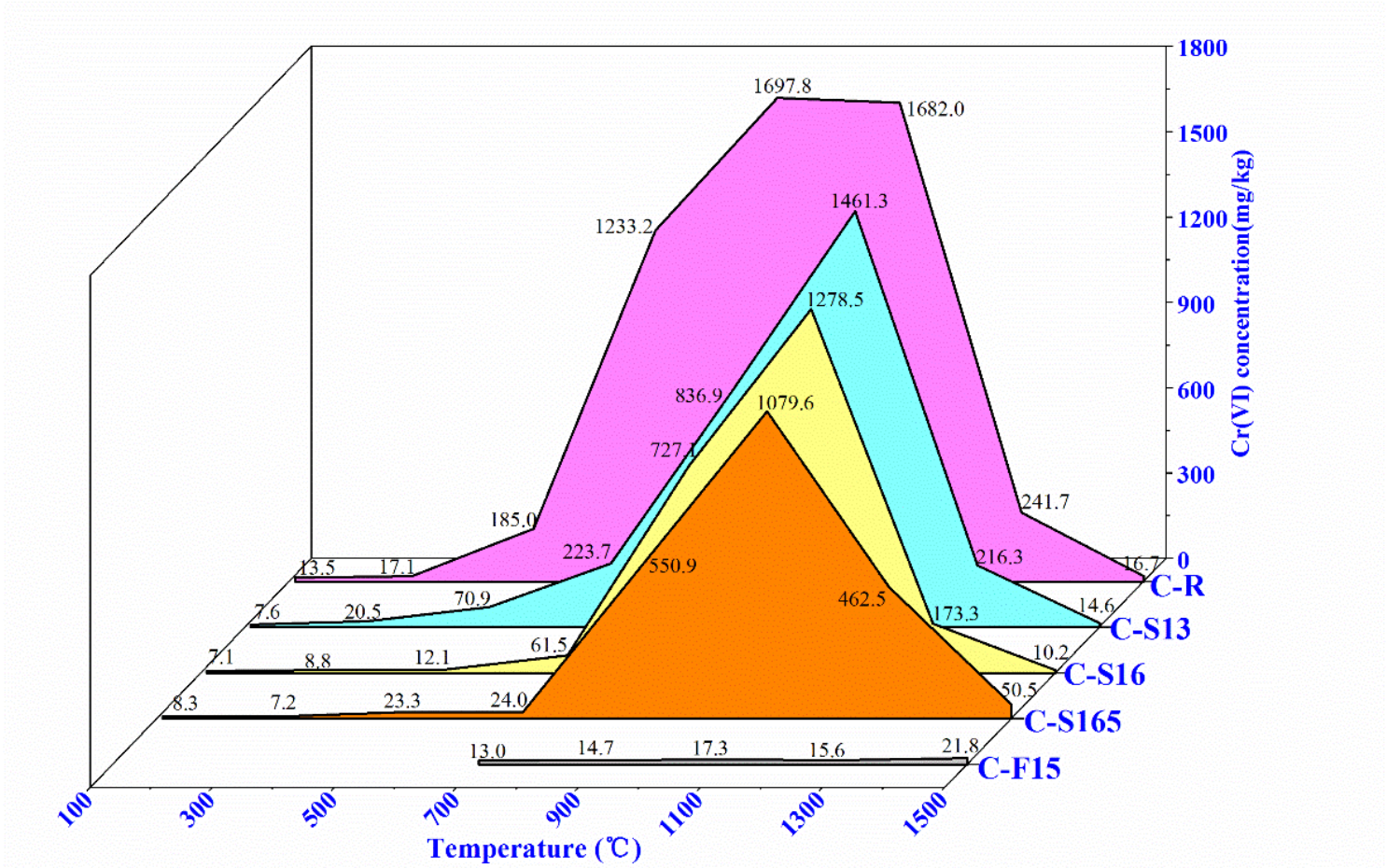

Figure 2

Cr(VI) concentration as a function of temperature in Al2O3-CaO-Cr2O3 castables.

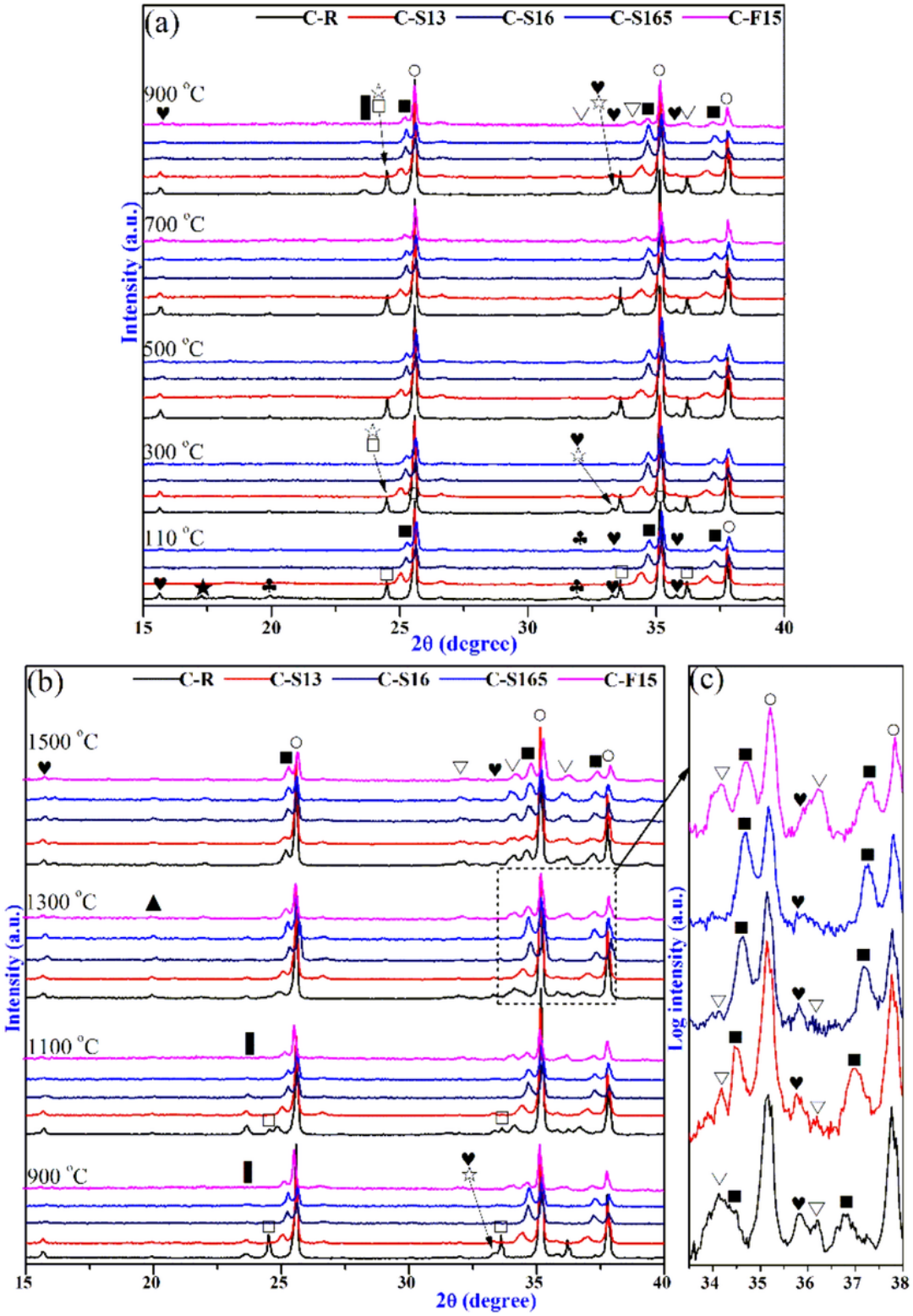

Figure 3

XRD patterns of Al2O3-CaO-Cr2O3 castables, (a) 110-900 oC, (b) 900-1500 oC, (c) 1300 oC. ●-Corundum (Al2O3), ■-(Al1-x,Crx)2O3 solid solution, □-Eskolaite (Cr2O3), ▯-CaCrO4, ▯-Hauyne (Ca4Al6CrO16), ▽-CA6 (CaAl12O19), ♥-NaAl11O17, ♣-C3AH6 (Ca3Al2(OH)12).

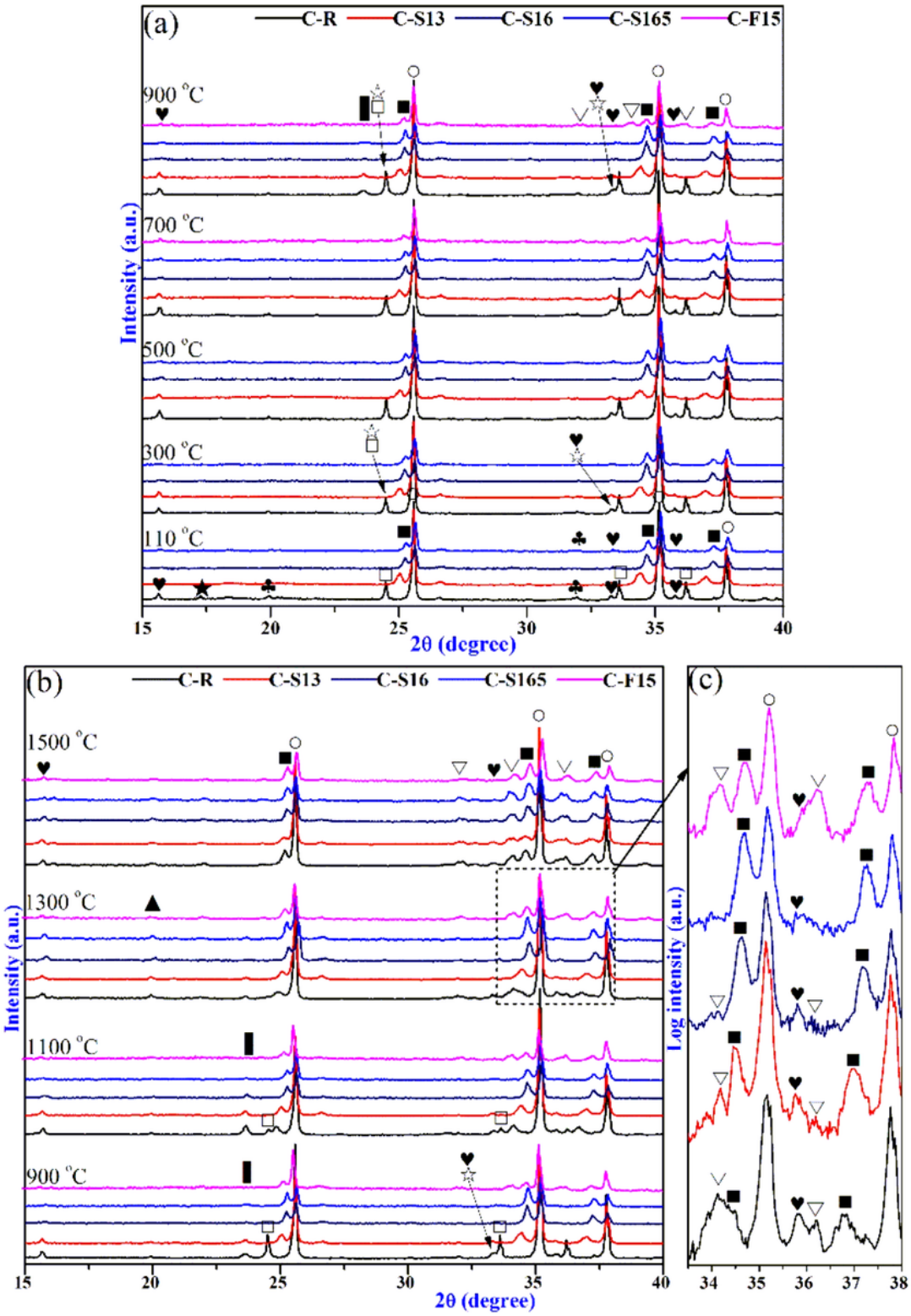

Figure 3

XRD patterns of Al2O3-CaO-Cr2O3 castables, (a) 110-900 oC, (b) 900-1500 oC, (c) 1300 oC. ●-Corundum (Al2O3), ■-(Al1-x,Crx)2O3 solid solution, □-Eskolaite (Cr2O3), ▯-CaCrO4, ▯-Hauyne (Ca4Al6CrO16), ▽-CA6 (CaAl12O19), ♥-NaAl11O17, ♣-C3AH6 (Ca3Al2(OH)12).

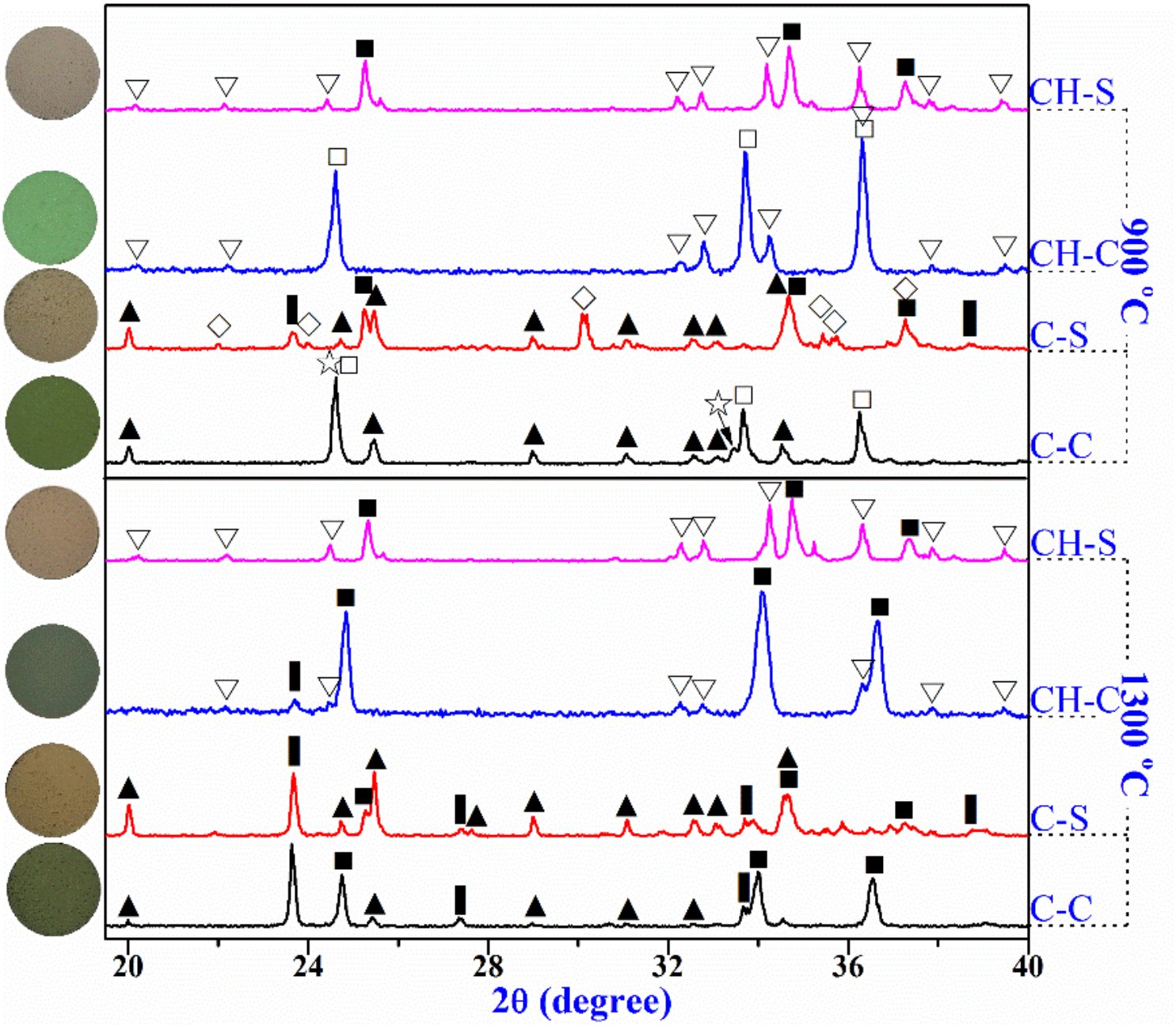

Figure 4

XRD pattern of cylindrical specimens heated at 900 oC and 1300 oC. ■-(Al1-x,Crx)2O3 solid solution. □-Eskolaite (Cr2O3), ▯-CaCrO4, ▯-Hauyne (Ca4Al6CrO16), ▲-CA2 (CaAl4O7), ▯-CA (CaAl2O4), ▽-CA6 (CaAl12O19).

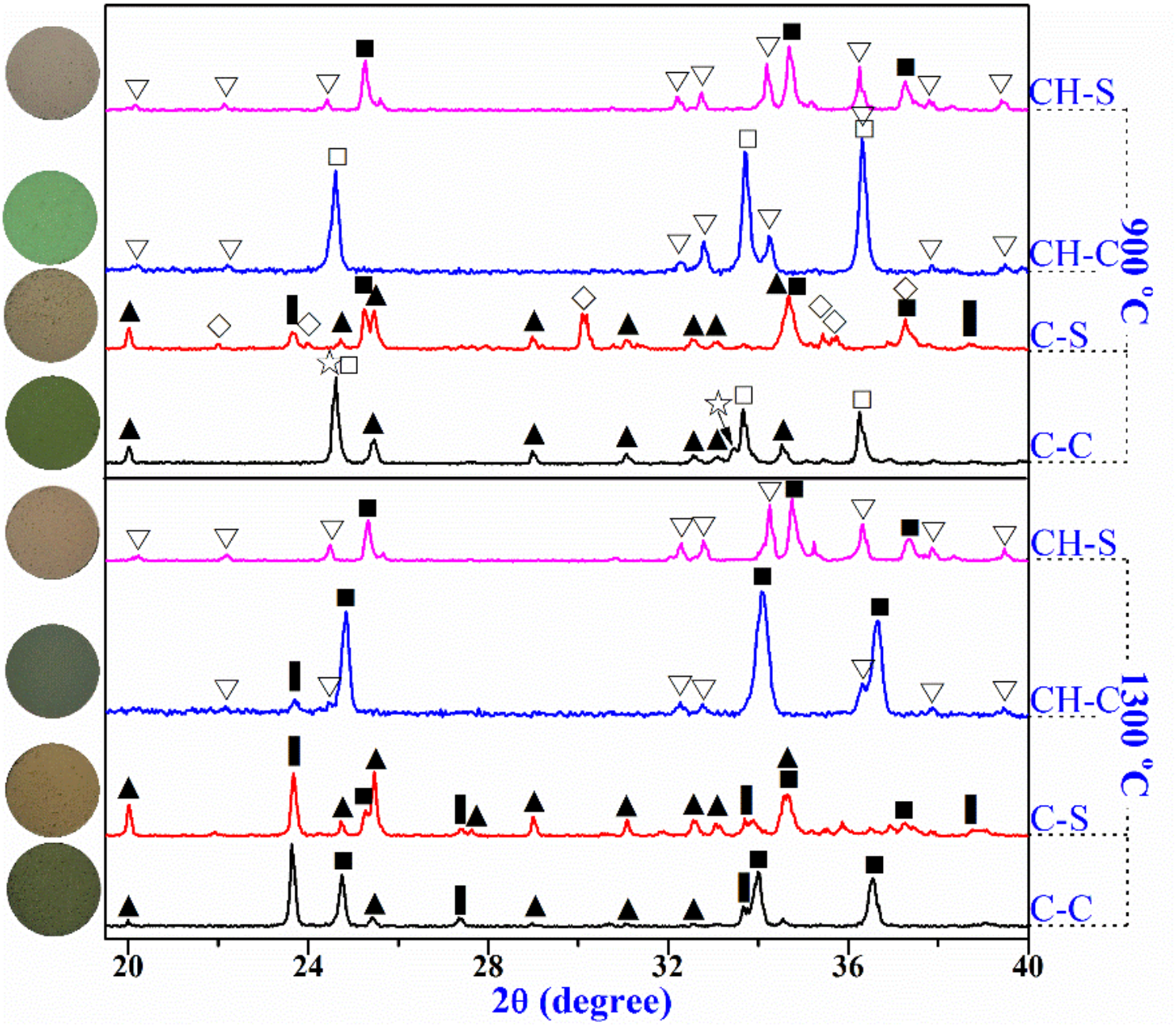

Figure 4

XRD pattern of cylindrical specimens heated at 900 oC and 1300 oC. ■-(Al1-x,Crx)2O3 solid solution. □-Eskolaite (Cr2O3), ▯-CaCrO4, ▯-Hauyne (Ca4Al6CrO16), ▲-CA2 (CaAl4O7), ▯-CA (CaAl2O4), ▽-CA6 (CaAl12O19).

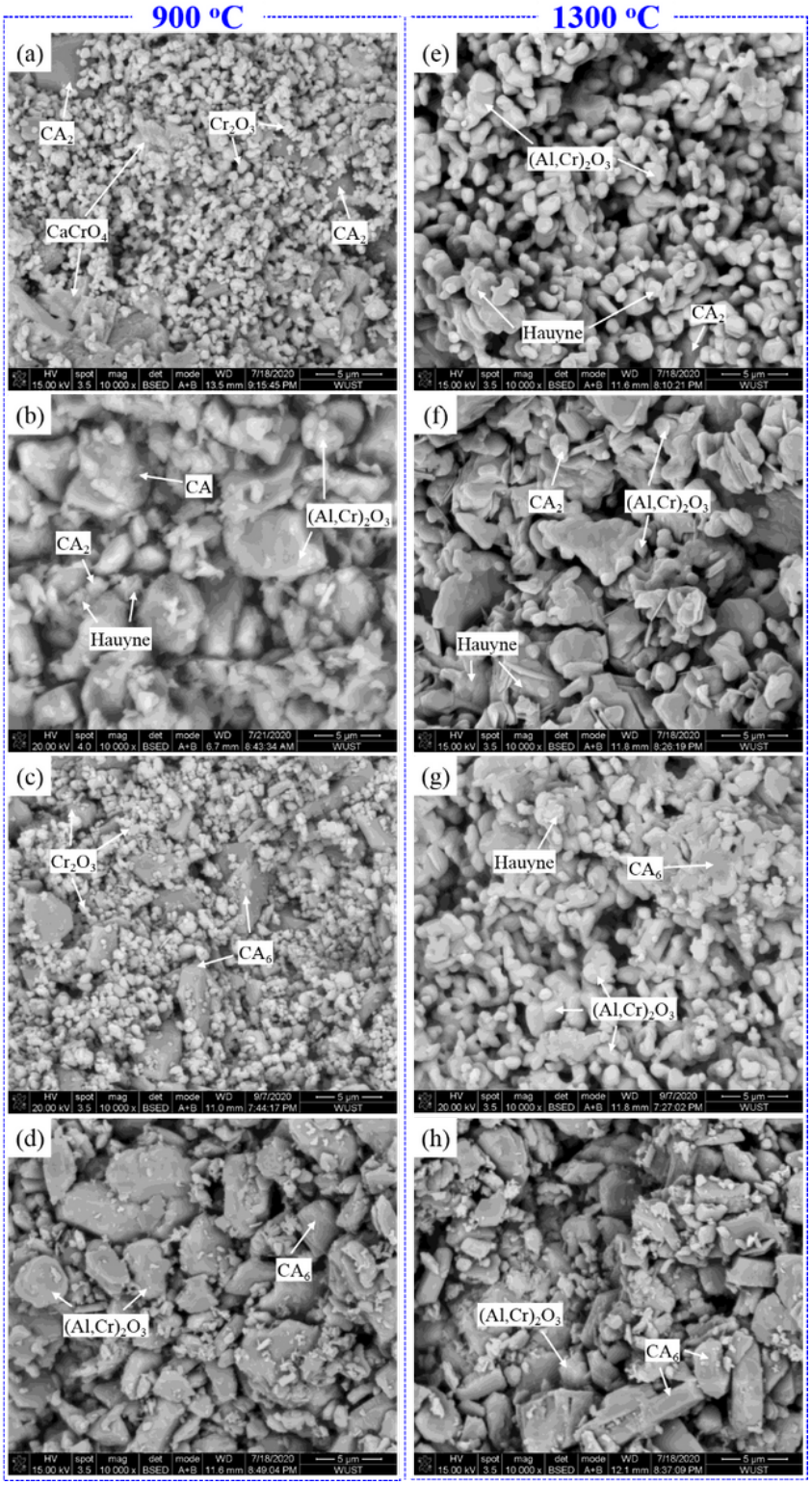

Figure 5

SEM images of cylindrical specimens heated at 900 oC and 1300 oC, (a) & (e) C-C, (b) & (f) C-S, (c) & (g) CH-C, (d) & (h) CH-S.

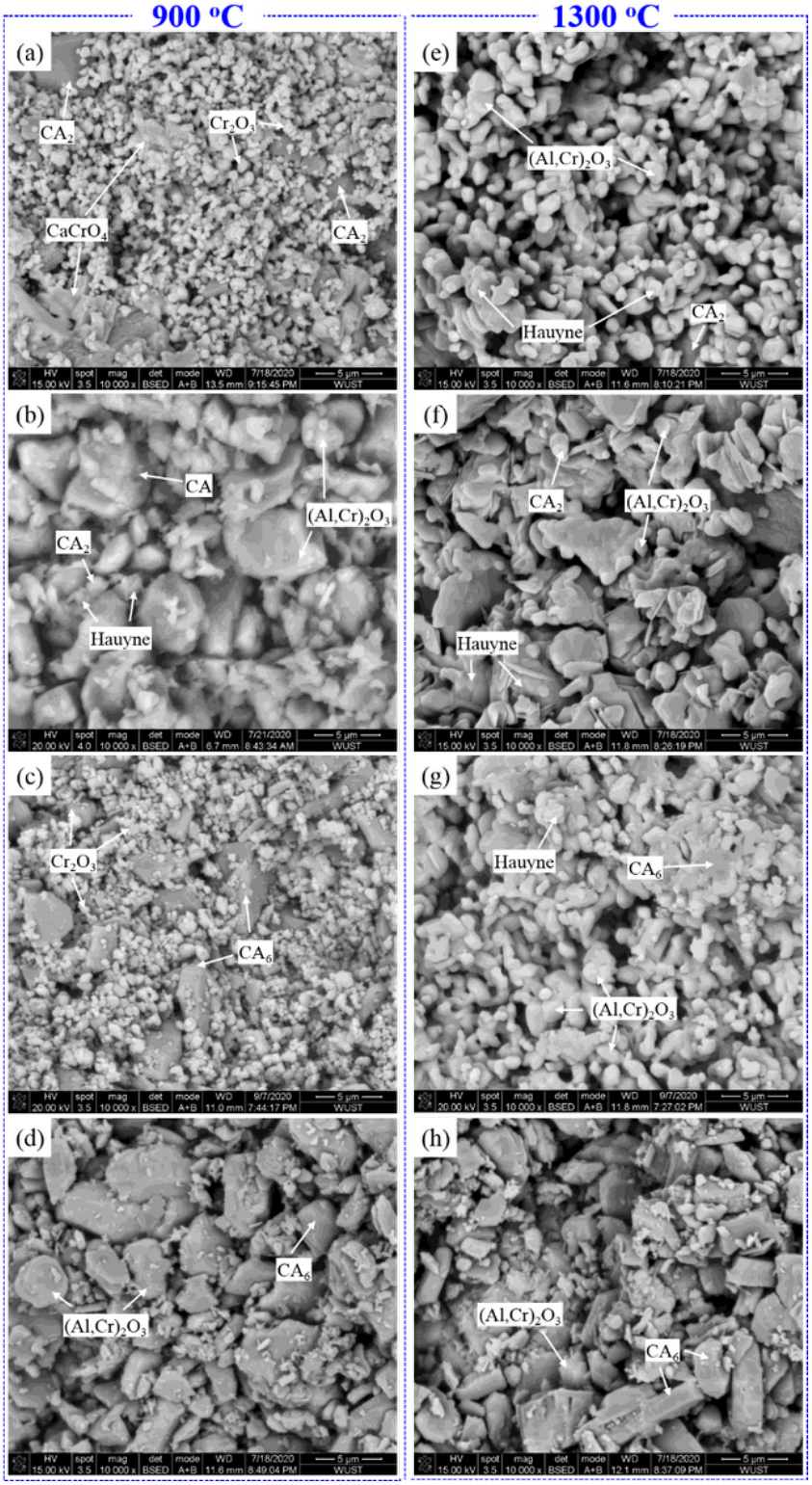

Figure 5

SEM images of cylindrical specimens heated at 900 oC and 1300 oC, (a) & (e) C-C, (b) & (f) C-S, (c) & (g) CH-C, (d) & (h) CH-S.